

Generation and structural characterization of aluminum cyanoacetylide

Carlos Cabezas,¹ Carmen Barrientos,² Antonio Largo,^{2,a)} Jean-Claude Guillemin,³ José Cernicharo,⁴ Isabel Peña,¹ and José L. Alonso^{1,a)}

¹*Grupo de Espectroscopia Molecular (GEM), Edificio Quifima, Laboratorios de Espectroscopia y Bioespectroscopia, Unidad Asociada CSIC, Parque Científico Uva, Universidad de Valladolid, Paseo de Belén 5, 47011 Valladolid, Spain*

²*Departamento de Química Física y Química Inorgánica, Facultad de Ciencias, Universidad de Valladolid, Campus Miguel Delibes, Paseo de Belén 7, 47011 Valladolid, Spain*

³*Institut des Sciences Chimiques de Rennes, École Nationale Supérieure de Chimie de Rennes, CNRS, UMR 6226, 11 Allée de Beaulieu, CS 50837, 35708 Rennes Cedex 7, France*

⁴*Group of Molecular Astrophysics, ICMM C/Sor Juana Ines de la Cruz N3 Cantoblanco, 28049 Madrid, Spain*

(Received 30 May 2014; accepted 19 August 2014; published online 8 September 2014)

Combined spectroscopy measurements and theoretical calculations bring to light a first investigation of a metallic cyanoacetylide, AlC_3N , using laser ablation molecular beam Fourier transform microwave spectroscopy. This molecule was synthesized in a supersonic expansion by the reaction of aluminum vapour with C_3N , produced from solid aluminum rods and BrCCCN in a newly constructed ablation-heating nozzle device. A set of accurate rotational and ^{27}Al and ^{14}N nuclear quadrupole coupling constants have been determined from the analysis of the rotational spectrum and compared with those predicted in a high-level *ab initio* study, conducting to the assignment of the observed species to linear AlCCCN . We have searched for this species towards the carbon-rich evolved star IRC + 10216 but only an upper limit to its abundance has been obtained. © 2014 AIP Publishing LLC. [<http://dx.doi.org/10.1063/1.4894501>]

I. INTRODUCTION

The nature of the metal-carbon chemical bonding in organometallic species has not been extensively explored, at least from a spectroscopic point of view, and it remains a topic of considerable interest. The experimentally determined molecular parameters of these molecules offer a unique opportunity to examine the competition between ionic and covalent bonding. Since these compounds play a wide range of roles in chemistry, establishing their structures provides a deeper understanding in, among others, catalytic processes and growth mechanisms of nanomaterials. Metal-bearing species are also of interest in astrochemistry. They were detected in space for the first time in the circumstellar envelope of the carbon-rich evolved star IRC + 10216.¹ Since then, the number of metal-bearing molecules detected in the interstellar medium has increased significantly. So far, the list of interstellar molecules includes species with Na, K, Mg, Al, and even transition metals such as Fe or Ti. In particular, among refractory species, aluminum-bearing molecules are predicted to be especially abundant according to recent studies.² Known interstellar aluminum-bearing molecules include halides (AlF ,^{1,3} AlCl^1), the oxide and hydroxide species (AlO ,⁴ AlOH^5), as well as aluminum isocyanide, AlNC .⁶ Other metal-containing cyanides and isocyanides have been observed in the interstellar medium. The list includes NaCN ,⁷ KCN ,⁸ MgNC ,⁹ MgCN ,¹⁰ and FeCN .¹¹ Silicon cyanide and

isocyanide have been also detected,^{12,13} and very recently the observation of a related magnesium molecule, HMgNC , was reported.¹⁴

The presence of a relatively wide variety of cyanides and isocyanides in space opens the possibility for the detection of longer carbon chains containing metals similar to the cyanopolyynes family: HC_3N , HC_5N , HC_7N , HC_9N , and HC_{11}N . In fact, HC_{11}N is the longest linear molecule observed in space¹⁵ so far. Analogue species containing metals could be synthesized through similar reaction schemes as those proposed for the family of cyanopolyynes.¹⁶ However, the possible detection of metal chains is hindered by the lack of spectroscopic information on these compounds. To the best of our knowledge none of these potential species have been characterized in laboratory.

In the present work we generated and characterized the first member of the Metal- C_3N series, containing aluminum and with formula AlC_3N . Laser ablation Fourier transform microwave spectroscopy (LA-MB-FTMW)¹⁷ has been used to generate AlC_3N and characterize its rotational spectrum across the 2–12 GHz frequency region. To conduct this study, a nozzle which combines a heating-reservoir with laser ablation capabilities has been developed, in order to employ solid precursors to generate the desired species. We have also carried out a complete computational study to guide the identification of the generated species. Finally, a search for the detected species has been performed towards IRC + 10216 but only upper limits have been derived. Experimental and computational strategies are described in Secs. II and III.

^{a)}Authors to whom correspondence should be addressed. Electronic addresses: alargo@qf.uva.es, Telephone: +34 983423482 and jlalonso@qf.uva.es, Telephone: +34 983186345.

II. EXPERIMENTAL

A. LA-MB-FTMW spectroscopy

The AlC_3N measurements were carried out using a new LA-MB-FTMW spectrometer¹⁸ constructed at the University of Valladolid specially designed to maximize performances at low frequency ranges (from 2 to 12 GHz). It has been recently employed in the studies of large biomolecules.^{18,19} In this investigation, our conventional ablation nozzle holder¹⁷ has been modified by addition of a home-made heatable reservoir extension, placed between the valve and the laser ablation nozzle. The reservoir can hold liquid and/or solid compounds that can be used as precursors of metal bearing species. This new device is accommodated in the backside of the fixed mirror, aligned parallel relative to the optical axis of the resonator.

Solid samples of BrCCCN were synthesized by bromination of cyanoacetylene as previously reported²⁰ (60 mmol (7.8 g) were obtained in one run starting from 0.1 mol of HC_3N and an aqueous Br^- - Br_2/KOH solution). The precursor was placed in the heatable reservoir to produce a jet expansion with enough concentration of cyanoacetylide. Hence, AlC_3N was created by laser ablation of aluminum rods in the throat of a pulsed supersonic expansion of Ne (10 bars stagnation pressure) and BrCCCN. A pulsed picosecond Nd:YAG-laser ($\lambda = 355$ nm and 10 mJ pulse⁻¹) at a repetition rate of 2 Hz was used. A motorized micrometer rotates and translates the sample rod each laser pulse, so the laser hits a different point of the sample surface in successive pulses, minimizing the problem of shot-to-shot fluctuation in the amount of the desorbed material.

Briefly, the sequence of an experimental cycle starts with a gas pulse of the mixing carrier gas (typically 450 μs). After an adequate delay, a laser pulse hits the metal rod, vaporizing the solid and producing plasma which trigger the chemical reactions in the precursor mixture.²¹ Immediately, the resulting products are supersonically expanded between the two mirrors of the Fabry–Pérot resonator and then a microwave pulse (0.3 μs) is applied, producing the macroscopic polarization of the species in the jet. Once the excitation ceases, molecular relaxation gives rise to a transient emission signal (free induction decay) at microwave frequencies, which is captured in the time domain. Its Fourier transformation to the frequency domain yields the rotational transitions that appear as Doppler doublets, because the supersonic jet travels parallel to the resonator axis. The molecular rest frequencies are calculated as the arithmetic mean of the Doppler doublets and are obtained with accuracy better than 3 kHz. Typically 100–200 pulses were accumulated to achieve an adequate signal-to-noise ratio.

B. Computational methods

We have carried out a survey of the AlC_3N potential hypersurface in order to characterize possible stable isomers. We are only aware of a previous theoretical study of AlC_3N isomers by Petrie,²² where just two isomers were considered. For our purpose we employed the second-order Møller-Plesset (MP2)²³ level of theory with Dunning's correlated consistent

triple-zeta basis sets augmented with diffuse and polarization functions, usually denoted as aug-cc-pVTZ.²⁴ Harmonic vibrational calculations were carried out for the stationary points obtained through this exploration in order to confirm that they correspond to true minima. For the more significant species characterized through this procedure we carried out subsequent CCSD(T) calculations²⁵ (coupled cluster with singles and doubles and a perturbative inclusion of triple excitations) with the aug-cc-pVTZ basis set.

In order to aid in the assignment of the rotational spectrum, reliable predictions for the rotational constant, as well as nuclear quadrupole coupling constants, are required. AlC_3N possesses two different nuclei with quadrupole moment, ²⁷Al ($I = 5/2$) and ¹⁴N ($I = 1$), which interact with the electric field gradient created by the rest of the molecule at the nucleus, splitting into a very complex hyperfine pattern each rotational transition. For the geometrical parameters two different procedures have been employed, CCSD(T) optimizations with Dunning's quadruple-zeta basis set, aug-cc-pVQZ and a composite procedure have been applied. This type of schemes at the coupled-cluster level has been developed by Gauss *et al.*^{26,27} A more affordable version of the method, in terms of computational demands, involving geometry optimizations at the MP2 level has been used by Barone *et al.*²⁸ as an alternative to expensive coupled-cluster calculations, showing also good results. In this context, we have also adopted this MP2-based composite method, to check its performance as an alternative to the expensive CCSD(T)/aug-cc-pVQZ that we have also carried out. For a detailed description of the method we refer to the paper of Barone *et al.*²⁸

Employing both theoretical procedures, CCSD(T)/aug-cc-pVQZ and the composite scheme, equilibrium spectroscopic parameters were obtained. In order to achieve an estimate of B_0 rotational constant, vibration-rotation interaction constants were estimated using second-order perturbation theory at the MP2/aug-cc-pVTZ level. Additionally, to aid in a possible experimental detection by IR spectroscopy, anharmonic vibrational frequencies and IR intensities have been predicted at that level of theory (Table S1 of the supplementary material⁴⁵). Both Gaussian 09²⁹ (MP2 geometries) and CFOUR³⁰ (CCSD(T) geometries) program packages were employed in this study.

III. RESULTS AND DISCUSSION

After exploring the AlC_3N potential hypersurface four linear isomers were obtained, namely AICCCN, AICCNC, AICNCC, and AINCCC (Figure 1). We also considered cyclic structures with aluminum in the middle of the chain. Thus, following the imaginary normal modes the optimization ended up with either CN-Al(C_2) and NC-Al(C_2). These two structures have an AlC_2 triangle subunit bonded to CN either through the nitrogen or the carbon atom, respectively. The relative energies of all these species, as well as their rotational constants and dipole moments obtained at the MP2/aug-cc-pVTZ level, are summarized in Table I, and the equilibrium bond distances for these isomers obtained at the same level are provided in Figure 1.

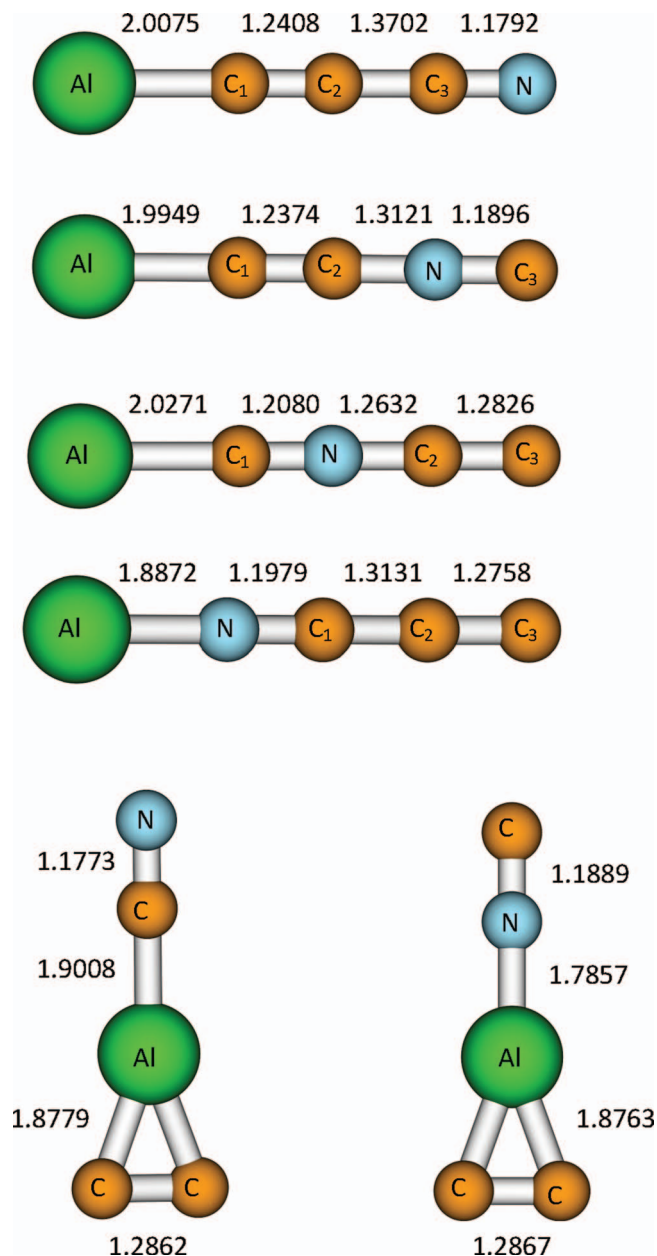


FIG. 1. Equilibrium geometrical parameters for the different AlC_3N isomers obtained at the MP2/aug-cc-pVTZ level. Distances are given in Angstroms.

TABLE I. Relative energies (kcal/mol) of the different AlC_3N species obtained at the MP2 and CCSD(T) levels with the aug-cc-pVTZ basis set. Zero-point vibrational energy (ZPVE) corrections are taken into account at the MP2/aug-cc-pVTZ level. Equilibrium rotational constants (MHz) and dipole moments (Debye) are estimated at the MP2/aug-cc-pVTZ level and CCSD/aug-cc-pVTZ levels, respectively.

Species	ΔE			A	B	C	μ
	$\Delta E(\text{MP2})$	$\Delta E(\text{CCSD(T)})$					
AlCCCN	0.0	0.0			1317.0		3.908
AlCCNC	30.66	26.04			1395.8		3.102
AlCNCC	65.18	66.23			1419.7		7.379
AlNCCC	24.71	22.07			1480.9		7.457
CN-Al(C_2)	29.1	25.58	50 875.0	2286.9	2188.5	2188.5	1.620
NC-Al(C_2)	25.4	25.68	50 914.0	2068.1	1987.4	1987.4	1.595

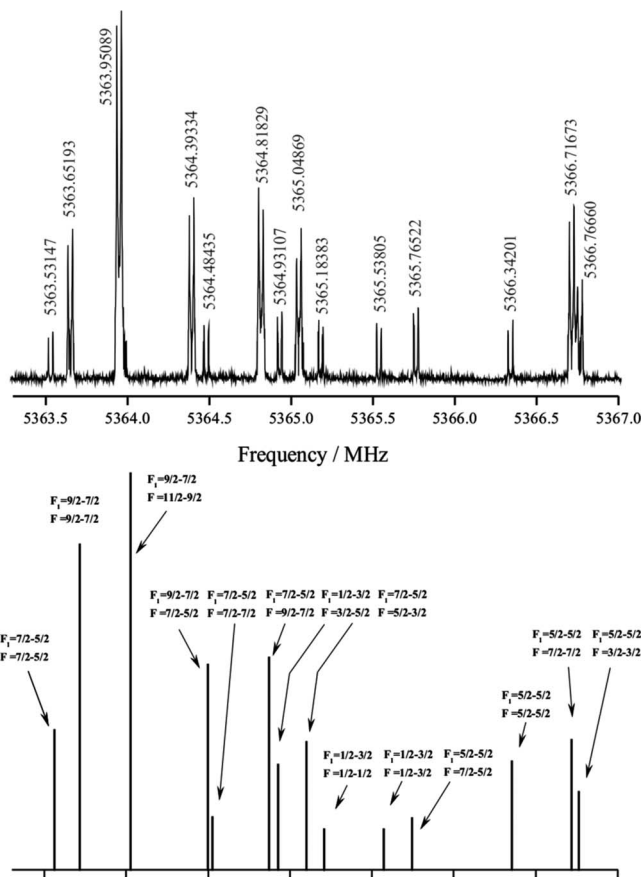


FIG. 2. (Upper panel) Central section of the $J = 2-1$ rotational transition of AlC_3N near 5.4 GHz. The nuclear quadrupole coupling hyperfine structure arising from both ^{27}Al ($I = 5/2$) and ^{14}N ($I = 1$) nuclei is clearly resolved. The coaxial arrangement of the adiabatic expansion and the resonator axis produces an instrumental Doppler doubling. The resonances frequencies are calculated as the average of the two Doppler components. (Lower panel) Theoretical simulation of the nuclear quadrupole hyperfine structure for the $J = 2-1$ rotational transition of AlCCCN isomer.

The energy results show that linear AlCCCN is the global minimum with the next lowest-lying isomer, namely AlNCCC, located more than 20 kcal/mol higher in energy. Because AlCCCN is the primary target for a possible experimental observation its geometrical parameters have been refined employing higher-level theoretical methods. In order to obtain more accurate predictions which can be useful for rotational spectroscopy, vibration-rotation interactions have been also estimated at the MP2/aug-cc-pVTZ level of theory and a correction of -3.7 MHz to the rotational constant has been found. After taking into account this correction the predicted rotational constant is 1329.2 MHz or 1337.9 MHz, at the CCSD(T)/aug-cc-pVTZ level and composite method, respectively.

On this basis, wide frequency scans from 5 to 6 GHz were directed to detect plausible signals corresponding to the $J = 2-1$ rotational transitions of the linear isomers of AlC_3N . A rotational transition centered around 5365 MHz, with a very complex hyperfine structure showing many fully resolved components (as shown in the upper panel of Figure 2) was finally found. The experimental value match nicely with that predicted by the composite method for the $J = 2-1$

TABLE II. Theoretical and experimental spectroscopic constants for Al-CCCN isomer. Theoretical rotational constants have been corrected with vibration-rotation interaction estimated at MP2/aug-cc-pVTZ level.

Parameter	Theoretical	Experimental
B (MHz)	1329.2 ^a / 1337.9 ^b	1340.757500 (32)
D (kHz)	0.0600 ^c	0.0673 (14)
eQq (Al) (MHz)	-38.224 ^d	-38.5993 (8)
eQq (N) (MHz)	-4.458 ^d	-4.2475 (6)
C ₁ (Al) (kHz)	...	1.257 (31)
rms (kHz)	...	0.6
N	...	73

^aCCSD(T)/aug-cc-pVQZ level.^bComposite method.^cMP2/aug-cc-pVTZ.^dCCSD/aug-cc-pVTZ.

transition of the linear AICCCN isomer at 5351 MHz. However, only a conclusive identification of the observed transition comes from the comparison between the predicted and observed nuclear quadrupole hyperfine structure. As can be seen in Figure 2, an exceptional matching exists between the observed and predicted spectra, when considering the eQq values for the ²⁷Al and ¹⁴N nuclei of Table II for the linear AICCCN isomer.

An initial fit,³¹ including the 27 hyperfine components measured for the $J = 2-1$ rotational transition gives rise a first set of constants which were used to predict and measure the $J = 1-0$, $J = 3-2$, and $J = 4-3$ centered at 2683, 8044, and 10 725 MHz, respectively. A total of 73 hyperfine components (collected in Table III) were analyzed³¹ using a ¹ Σ Hamiltonian of the following form:³² $H = H_R + H_Q + H_{nsr}$ where H_R contains rotational and centrifugal distortion parameters, H_Q the quadrupole coupling interactions while H_{nsr} describes the nuclear spin-rotation terms. The energy levels involved in each transition are labeled with the quantum numbers J , F_1 , and F , where $F_1 = J + I_{Al}$ and $F = F_1 + I_N$. The experimental values for the rotational parameters B_0 and D , the electric quadrupole coupling constant eQq for the ²⁷Al and ¹⁴N nuclei along with the nuclear spin-rotation parameter C_1 (²⁷Al) for the aluminum nucleus were derived from the analysis. Attempting to fit this last constant for the ¹⁴N nucleus resulted in values that were undefined to within their 3σ uncertainties. The standard deviation obtained for the fit is 0.6 kHz. Confirmation of the observed species as the linear AICCCN isomer resides in the excellent agreement between the experimental and theoretical values of the rotational and ²⁷Al and ¹⁴N nuclear quadrupole coupling constants collected in Table II.

Additional searches to find rotational signatures of other species of AIC₃N failed. At this point, it is interesting to note that both aluminum cyanide and isocyanide have been experimentally observed by rotational spectroscopy,^{33,34} being AINC predicted to be about 5 kcal/mol more stable than AICN.^{35,36} BrCCCN can be considered as a good generator of Metal-CCCN species but it might not be suitable for generating M-NCCC species, which is an important issue to consider in the non-observation of AINCCC in our experiment. In addition, in the case of AIC₃N species the cyanide isomer is

TABLE III. Measured frequencies and residuals (in MHz) for the nuclear quadrupole coupling hyperfine components of AICCCN.

J'	J''	F'_1	F''_1	F'	F''	$\nu_{obs.}$	$\nu_{obs.} - \nu_{calc.}$		
1	0	2.5	2.5	1.5	1.5	2674.63471	-0.00049		
		2.5	2.5	3.5	3.5	2675.05122	-0.00046		
		2.5	2.5	2.5	2.5	2676.00137	-0.00024		
		3.5	2.5	3.5	2.5	2682.89096	-0.00029		
		3.5	2.5	2.5	1.5	2683.57333	-0.00196		
		3.5	2.5	4.5	3.5	2683.66385	-0.00011		
		1.5	2.5	1.5	1.5	2686.77891	-0.00138		
		1.5	2.5	0.5	1.5	2687.13311	-0.00050		
		1.5	2.5	2.5	3.5	2687.41089	-0.00059		
		2	1	2.5	1.5	1.5	0.5	5354.26762	-0.00106
				2.5	1.5	3.5	2.5	5354.35676	0.00020
				2.5	1.5	2.5	2.5	5354.93291	-0.00076
				2.5	1.5	2.5	1.5	5355.56552	-0.00025
				3.5	3.5	2.5	2.5	5356.10914	0.00042
				3.5	3.5	4.5	4.5	5356.20544	0.00001
				3.5	3.5	3.5	3.5	5356.64182	-0.00018
3.5	2.5			3.5	2.5	5363.53147	-0.00017		
4.5	1.5			3.5	2.5	5360.55638	-0.00009		
4.5	3.5			4.5	3.5	5363.65193	0.00049		
1.5	1.5			2.5	1.5	5360.44958	-0.00053		
1.5	1.5			1.5	2.5	5360.50497	-0.00007		
1.5	1.5			1.5	0.5	5360.78391	0.00008		
4.5	3.5			5.5	4.5	5363.95089	0.00037		
1.5	1.5			1.5	1.5	5361.13692	-0.00022		
4.5	3.5			3.5	2.5	5364.39334	-0.00023		
3.5	2.5	3.5	3.5	5364.48435	0.00064				
3.5	2.5	4.5	3.5	5364.81829	0.00058				
0.5	1.5	1.5	2.5	5364.93107	0.00021				
3.5	2.5	2.5	1.5	5365.04869	-0.00012				
0.5	1.5	0.5	0.5	5365.18383	-0.00009				
0.5	1.5	0.5	1.5	5365.53805	0.00081				
2.5	2.5	3.5	2.5	5365.76522	0.00093				
2.5	2.5	2.5	2.5	5366.34201	0.00061				
2.5	2.5	3.5	3.5	5366.71673	0.00037				
2.5	2.5	1.5	1.5	5366.76660	-0.00049				
2.5	2.5	2.5	3.5	5367.29364	0.00017				
3	2	4.5	4.5	5.5	5.5	8037.77458	0.00109		
		1.5	0.5	2.5	1.5	8041.00381	0.00079		
		2.5	1.5	2.5	1.5	8041.06585	-0.00021		
		2.5	1.5	3.5	2.5	8041.68165	0.00057		
		3.5	2.5	3.5	2.5	8042.11209	0.00081		
		2.5	1.5	1.5	0.5	8042.15330	0.00041		
		4.5	2.5	3.5	2.5	8043.70899	-0.00040		
		3.5	2.5	2.5	1.5	8043.78790	0.00070		
		3.5	2.5	4.5	3.5	8043.81635	-0.00030		
		5.5	4.5	5.5	5.5	8043.82945	-0.00101		
		4.5	3.5	4.5	4.5	8044.50608	-0.00075		
		3.5	3.5	3.5	2.5	8044.77355	0.00022		
		4.5	3.5	4.5	3.5	8044.84035	-0.00048		
		5.5	4.5	5.5	4.5	8044.90024	0.00014		
		5.5	4.5	4.5	3.5	8044.98067	0.00003		
		4.5	3.5	5.5	4.5	8045.51866	0.00008		
1.5	1.5	1.5	1.5	8045.67326	0.00124				
1.5	1.5	2.5	2.5	8046.11592	0.00005				
4.5	3.5	3.5	2.5	8046.37197	0.00053				
4.5	3.5	3.5	3.5	8046.51845	-0.00070				
2.5	2.5	2.5	2.5	8046.63682	-0.00061				
2.5	2.5	3.5	3.5	8047.14293	0.00040				
2.5	2.5	1.5	1.5	8047.23619	-0.00079				
2.5	3.5	2.5	3.5	8049.44645	-0.00074				

TABLE III. (Continued.)

J'	J''	F'_1	F''_1	F'	F''	$\nu_{\text{obs.}}$	$\nu_{\text{obs.}} - \nu_{\text{calc.}}$
4	3	2.5	1.5	2.5	1.5	10 724.05291	-0.00040
		3.5	2.5	3.5	2.5	10 724.49903	0.00018
	2.5	1.5	3.5	2.5	10 724.69515	-0.00129	
	3.5	2.5	4.5	3.5	10 724.98315	0.00030	
	1.5	0.5	2.5	1.5	10 725.34913	0.00028	
	4.5	3.5	4.5	3.5	10 725.73774	-0.00044	
	1.5	0.5	0.5	0.5	10 725.74059	-0.00014	
	4.5	3.5	3.5	2.5	10 725.88506	-0.00013	
	4.5	3.5	5.5	4.5	10 726.00496	0.00018	
	4.5	4.5	5.5	5.5	10 726.20217	0.00066	
	5.5	4.5	5.5	4.5	10 726.25886	-0.00028	
	6.5	5.5	5.5	4.5	10 726.32945	0.00095	
	5.5	4.5	4.5	3.5	10 726.37781	-0.00059	

20 kcal/mol more stable than the isocyanide isomer. Hence, although AlNCCC was actually generated in our experiment it would not be enough populated to be detected.

The electronic quadrupole coupling constant for the Al nucleus was found to be $eQq(\text{Al}) = -38.5993$ (8) MHz. This value can be compared with those for other aluminum containing species to gain some insights about the bonding properties of Al-C union. The quadrupole constant of AICCCN lies between those for AICCH (-42.3917 (65) MHz)²¹ and AICN (-37.2225 (29) MHz).³³ These numbers suggest that the bond Al-C in AICCCN is not as covalent as AICCH and presents some ionic character like in the AICN system. This fact is reflected in the Al-C bond lengths, shown in Table IV. The previous conclusion has been confirmed by using a topological analysis of the electronic density in the framework of the Bader's Quantum Theory of Atoms in Molecules (QTAIM).³⁸ This analysis was performed for each stationary point on the PES's using the Keith's AIMAll package³⁹ including standard thresholds. Results for AICN, AICCCN, and AICCH are shown in Table V and the corresponding contour maps of the Laplacian of the electron density are shown in Figure S1 of the supplementary material.⁴⁵ In this context two limiting types of interactions can be identified namely shared and closed-shells interactions.⁴⁰ In shared interactions, typical of covalent compounds, the nuclei are bound as a consequence of the lowering of the potential energy associated with the concentration of electronic charge shared between the nuclei; this is reflected in relatively large values of $\rho(r)$ and negative values of the Laplacian, $\nabla^2\rho(r)$ at the critical point. The

TABLE IV. Nuclear quadrupole coupling constant for the Al nucleus and Al-C bond distances for some Al-containing species.

Species	$eQq(\text{Al})$ (MHz)	Al-C (\AA)
AICCH	-42.3917 (65) ^a	1.986 ^b
AICCCN	-38.5993 (8) ^c	2.008 ^d
AICN	-37.2225 (29) ^e	2.015 ^f

^aReference 21.

^bReference 37.

^cThis work.

^dTheoretical value of this work.

^eReference 33.

^fTheoretical value from Ref. 35.

TABLE V. Local topological properties (in a.u.) of the electronic charge density distribution calculated at the position of the bond critical points for the different (AIMAll) species.^a

Species	Bond	$\rho(r)$	$\nabla^2\rho(r)$	$ V(r) /G(r)$	$H(r)$
AICN	Al-C	0.069	0.242	1.214	-0.016
	C-N	0.487	-0.457	2.142	-0.919
AICCCN	Al-C ₁	0.072	0.266	1.205	-0.017
	C ₁ -C ₂	0.413	-1.357	3.018	-0.672
	C ₂ -C ₃	0.313	-1.043	4.488	-0.366
	C ₃ -N	0.482	-0.333	2.102	-0.898
AICCH	Al-C ₁	0.075	0.289	1.204	-0.019
	C ₁ -C ₂	0.410	-1.350	3.058	-0.657
	C ₂ -H	0.299	-1.253	10.458	-0.350

^aThe electronic charge density [$\rho(r)$], the Laplacian [$\nabla^2\rho(r)$], the relationship between the potential energy density $V(r)$ and the lagrangian form of kinetic energy density $G(r)$ and the total energy density, $|H(r)|$.

second limiting type of atomic interaction is that occurring between closed-shell systems, such as those found in ionic bond or van der Waals molecules for instance. In these interactions, $\rho(r)$ is relatively low in value and the Laplacian, $\nabla^2\rho(r)$, is positive.

Another useful property to characterize the degree of covalence of a bond is the total energy density $H(r)$. It is defined as the sum of the potential energy density, $V(r)$ and the gradient kinetic energy density $G(r)$ at a critical point. In covalent interactions $H(r)$ is negative in value⁴¹ and the positive value of $H(r)$ is characteristic of ionic interactions and van der Waals systems.⁴⁰ The covalent character of an interaction can also be quantitatively analyzed by taking into account the $|V(r)|/G(r)$ ratio. In covalent interactions the value of this relationship is greater than 2. It is smaller than 1 for non-covalent interactions and between 1 and 2 for partially covalent bonds.

The local topological properties of the carbon-carbon and carbon-nitrogen bond critical points are indicative of shared interactions: large values of electron density, negative values of its Laplacian, $|V(r)|/G(r)$ ratios greater than 2 and negative values of the total energy densities $H(r)$. On the opposite, the aluminum-carbon bond critical points show low values of $\rho(r)$ and positive values of its Laplacian. The $|V(r)|/G(r)$ ratios are between 1 and 2 and $H(r)$ is negative with a low value. Thus these interactions can be classified as closed shell interactions (typical of ionic compounds) with a small degree of covalence.

On the other hand, the quasi identical eQq values for ¹⁴N nucleus in AICCCN and HCCCN, -4.2475 (6) MHz and -4.31924 (1) MHz⁴² respectively, indicate that the electronic environment around the ¹⁴N nucleus is very similar in both species. Thus, one can infer that the nature of the bond in the C≡N group in AICCCN should be the same to that found in HCCCN.

Finally, the rotational constants derived from the observed laboratory spectrum of AICCCN allow performing a search in the millimeter domain using the 3 mm line survey of IRC + 10216 taken with the 30-m IRAM radiotelescope.^{43,44} The values of the experimental constants obtained in the present investigation have been used to predict its transitions

in the 3 mm domain with uncertainties of 0.15–0.4 MHz, which is enough to search for lines having total frequency coverage in IRC + 10216 of ~ 10 MHz at these frequencies (total linewidth ~ 29 km/s). Unfortunately, we have not detected any of the lines covered in the line survey, from $J = 30$ – 29 up to $J = 43$ – 42 . From the most sensitive spectra we obtain an upper limit (3σ) to the column density of AICCCN in front of IRC + 10216 of $< 3 \times 10^{12}$ cm $^{-2}$. Note that, AINC has been detected⁶ in this source with a column density of 9×10^{11} cm $^{-2}$. The upper limit obtained for the column density of AICCCN is 3 times higher than that of AINC. Although the dipole moment of AICCCN is higher than that of AINC, its partition function is much higher and it could be much better to search for this species in the 7 mm domain.

IV. CONCLUSIONS

The first metal cyanoacetylide, AICCCN, has been produced and characterized in the laboratory using a combination of laser ablation techniques and Fourier transform microwave spectroscopy. A newly constructed ablation-heating source has been proved as an effective method to create metallic cyanoacetylides, using solid samples of BrCCCN as main precursor.

The predictions for the rotational constant at both CCSD(T)/aug-cc-pVQZ and composite methods are in good agreement with the experimental value. Since the composite method is more affordable in terms of computational demands than the CCSD(T)/aug-cc-pVQZ level, our results suggest that the composite method corrected with vibration-rotation interaction can provide good estimates of rotational constants for this type of compounds.

We have searched for AICCCN species towards the carbon-rich evolved star IRC + 10216 and obtained only upper limits. Important information on the chemistry of metal cyanides and isocyanides could be obtained if M-CCCN species are detected in the circumstellar medium. Mg- and Na-C₃N are the most obvious candidates after AIC₃N and will be studied soon in our laboratory. Although their detection seems to be difficult within the state-of-the-art observations of evolved stars, the sensitivity that will be provided by the ALMA interferometer in the next years could open the possibility to detect these species in circumstellar envelopes.

ACKNOWLEDGMENTS

This research has been supported by the Ministerio de Ciencia e Innovación of Spain (Grants CTQ2010-19008, Consolider-Ingenio 2010 CSD2009-00038, and CTQ2010-16864), by European Research Council under the European Union's Seventh Framework Programme (FP/2007-2013)/ERC-2013-SyG (Grant Agreement No. 610256 NANOCOSMOS) and by the Junta de Castilla y León (Grants VA175U13 and VA077U13). C.C. thanks the Junta de Castilla y León for a postdoctoral contract (Grant CIP13/01). J.-C.G. thanks the Centre National d'Etudes Spatiales (CNES) and the Program PCMI (INSU-CNRS) for financial support. J.-C.G. and J.C. received the support of the contract

ANR-13-BS05-0008 IMOLABS. We thank Marcelino Agúndez for useful comments and suggestions.

- ¹J. Cernicharo and M. Guélin, *Astron. Astrophys.* **183**, L10 (1987).
- ²M. Agúndez, J. P. Fonfría, J. Cernicharo, C. Kahane, F. Daniel, and M. Guélin, *Astron. Astrophys.* **543**, A48 (2012).
- ³L. M. Ziurys, A. J. Apponi, and T. G. Phillips, *Astrophys. J.* **433**, 729 (1994).
- ⁴E. D. Tenenbaum and L. M. Ziurys, *Astrophys. J.* **694**, L59 (2009).
- ⁵E. D. Tenenbaum and L. M. Ziurys, *Astrophys. J.* **712**, L93 (2010).
- ⁶L. M. Ziurys, C. Savage, J. L. Highberger, A. J. Apponi, M. Guélin, and J. Cernicharo, *Astrophys. J.* **564**, L45 (2002).
- ⁷B. E. Turner, T. C. Steimle, and L. Meerts, *Astrophys. J.* **426**, 97 (1994).
- ⁸R. L. Pulliam, C. Savage, M. Agúndez, J. Cernicharo, M. Guélin, and L. M. Ziurys, *Astrophys. J.* **725**, L181 (2010).
- ⁹K. Kawaguchi, E. Kagi, T. Hirano, S. Takano, and S. Saito, *Astrophys. J.* **406**, L39 (1993).
- ¹⁰L. M. Ziurys, A. J. Apponi, M. Guélin, and J. Cernicharo, *Astrophys. J.* **445**, L47 (1995).
- ¹¹L. N. Zack, D. T. Halfen, and L. M. Ziurys, *Astrophys. J.* **733**, L36 (2011).
- ¹²M. Guélin, S. Muller, J. Cernicharo, A. J. Apponi, M. C. McCarthy, C. A. Gottlieb, and P. Thaddeus, *Astron. Astrophys.* **363**, L9 (2000).
- ¹³M. Guélin, S. Muller, J. Cernicharo, M. C. McCarthy, and P. Thaddeus, *Astron. Astrophys.* **426**, L49 (2004).
- ¹⁴C. Cabezas, J. Cernicharo, J. L. Alonso, M. Agúndez, S. Mata, M. Guélin, and I. Peña, *Astrophys. J.* **775**, 133 (2013).
- ¹⁵M. B. Bell, P. A. Feldman, M. J. Travers, M. C. McCarthy, C. A. Gottlieb, and P. Thaddeus, *Astrophys. J.* **483**, L61 (1997).
- ¹⁶E. Herbst, *Chem. Soc. Rev.* **30**, 168 (2001).
- ¹⁷J. L. Alonso, C. Pérez, M. E. Sanz, J. C. López, and S. Blanco, *Phys. Chem. Chem. Phys.* **11**, 617 (2009) and references therein.
- ¹⁸C. Bermúdez, S. Mata, C. Cabezas, and J. L. Alonso, *Angew. Chem., Int. Ed.* **53**, 6655 (2014).
- ¹⁹M. E. Sanz, C. Cabezas, S. Mata, and J. L. Alonso, *J. Chem. Phys.* **140**, 204308 (2014).
- ²⁰E. Kloster-Jensen, *Acta Chem. Scand.* **17**, 1862–1865 (1963).
- ²¹C. Cabezas, S. Mata, A. M. Daly, A. Martín, J. L. Alonso, and J. Cernicharo, *J. Mol. Spectrosc.* **278**, 31 (2012).
- ²²S. Petrie, *Mon. Not. R. Astron. Soc.* **302**, 482 (1999).
- ²³C. Møller and M. Plesset, *Phys. Rev.* **46**, 618 (1934).
- ²⁴T. H. Dunning, *J. Chem. Phys.* **90**, 1007 (1989).
- ²⁵K. Raghavachari, G. W. Trucks, J. A. Pople, and M. Head-Gordon, *Chem. Phys. Lett.* **157**, 479 (1989).
- ²⁶M. Heckert, M. Kalay, and J. Gauss, *Mol. Phys.* **103**, 2109 (2005).
- ²⁷M. Heckert, M. Kalay, D. P. Tew, W. Klopper, and J. Gauss, *J. Chem. Phys.* **125**, 044108 (2006).
- ²⁸V. Barone, M. Biczysko, J. Bloino, and C. Puzzarini, *J. Chem. Theory Comput.* **9**, 1533 (2013).
- ²⁹M. J. Frisch, G. W. Trucks, H. B. Schlegel *et al.* Gaussian 09, Revision B.01, Gaussian, Inc., Wallingford, CT, 2010.
- ³⁰CFOUR, a quantum chemical program package written by J. F. Stanton, J. Gauss, M. E. Harding, and P. G. Szalay with contributions from A. Auer, R. J. Bartlett, U. Benedikt, C. Berger, D. E. Bernholdt, Y. J. Bomble, L. Cheng, O. Christiansen, M. Heckert, O. Heun, C. Huber, T.-C. Jagau, D. Jonsson, J. Jusélius, K. Klein, W. J. Lauderdale, D. A. Matthews, T. Metzroth, L. A. Mück, D. P. O'Neill, D. R. Price, E. Prochnow, C. Puzzarini, K. Ruud, F. Schiffmann, W. Schwalbach, C. Simmons, S. Stopkowitz, A. Tajti, J. Vázquez, F. Wang, J. D. Watts and the integral packages MOLECULE (J. Almlöf and P. R. Taylor), PROPS (P. R. Taylor), ABACUS (T. Helgaker, H. J. Aa. Jensen, P. Jørgensen, and J. Olsen), and ECP routines by A. V. Mitin and C. van Wüllen, 2013.
- ³¹H. M. Pickett, *J. Mol. Spectrosc.* **148**, 371 (1991).
- ³²W. Gordy and R. L. Cook, *Microwave Molecular Spectra*, 3rd ed. (Wiley, New York, 1984).
- ³³K. A. Walker and M. C. L. Gerry, *Chem. Phys. Lett.* **301**, 200 (1999).
- ³⁴J. S. Robinson, A. J. Apponi, and L. M. Ziurys, *Chem. Phys. Lett.* **278**, 1 (1997).
- ³⁵B. Ma, Y. Yamaguchi, and H. F. Schaefer III, *Mol. Phys.* **86**, 1331 (1995).
- ³⁶S. Petrie, *J. Phys. Chem.* **100**, 11581 (1996).
- ³⁷M. Sun, D. T. Halfen, D. J. Clouthier, and L. M. Ziurys, *Chem. Phys. Lett.* **553**, 11–16 (2012).
- ³⁸R. W. F. Bader, *Atoms in Molecules: A Quantum Theory* (Clarendon Press, New York, 1990).

- ³⁹T. A. Keith, AIMAll, version 13.11.04, Professional, TK Gristmill Software: Overland Park, KS, 2013, see <http://aim.tkgristmill.com>.
- ⁴⁰R. W. F. Bader, *Chem. Rev.* **91**, 893–928 (1991).
- ⁴¹D. Cremer and E. Kraka, *Angew. Chem., Int. Ed.* **23**, 627–628 (1984).
- ⁴²R. L. DeLeonb and J. S. Muentner, *J. Chem. Phys.* **82**, 1702 (1985).
- ⁴³J. Cernicharo, M. Guélin, M. Agúndez, M. C. McCarthy, and P. Thaddeus, *Astrophys. J.* **688**, L83–L86 (2008).
- ⁴⁴Cernicharo *et al.* “A sensitive line survey at 3 mm with the 30 m IRAM radio telescope of IRC+10216” (unpublished).
- ⁴⁵See supplementary material at <http://dx.doi.org/10.1063/1.4894501> for Table S1, with the anharmonic vibrational frequencies and IR intensities for AICCCN evaluated at the MP2/aug-cc-pVTZ level and Figure S1, with the contour maps of the Laplacian distribution of the electron density for the AICN, AICCCN, and AICCH species.